Neurobiology of Aging 76 (2019) 141–150

Contents lists available at ScienceDirect

Neurobiology of Aging

journal homepage: www.elsevier.com/locate/neuaging

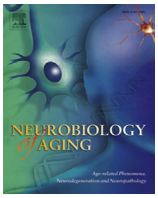

Amyloid deposition is associated with different patterns of hippocampal connectivity in men versus women

Minjie Wu[a], Rebecca C. Thurston[a,b], Dana L. Tudorascu[c], Helmet T. Karim[a], Chester A. Mathis[d], Brian J. Lopresti[d], M. Ilyas Kamboh[e], Ann D. Cohen[a], Beth E. Snitz[f], William E. Klunk[a], Howard J. Aizenstein[a,g,*]

[a] Department of Psychiatry, University of Pittsburgh, Pittsburgh, PA, USA
[b] Departments of Epidemiology and Psychology, University of Pittsburgh, Pittsburgh, PA, USA
[c] Departments of Medicine and Biostatistics, University of Pittsburgh, Pittsburgh, PA, USA
[d] Department of Radiology, University of Pittsburgh, Pittsburgh, PA, USA
[e] Department of Human Genetics, University of Pittsburgh, Pittsburgh, PA, USA
[f] Department of Neurology, University of Pittsburgh, Pittsburgh, PA, USA
[g] Department of Bioengineering, University of Pittsburgh, Pittsburgh, PA, USA

ARTICLE INFO

Article history:
Received 15 February 2018
Received in revised form 4 October 2018
Accepted 18 November 2018
Available online 1 December 2018

Keywords:
Alzheimer's disease
Gender
Beta-amyloid
Functional connectivity
Neural compensation

ABSTRACT

Compared to men, women are disproportionally affected by Alzheimer's disease (AD) and have an accelerated trajectory of cognitive decline and disease progression. Neurobiological factors underlying gender differences in AD remain unclear. This study investigated brain beta-amyloid (Aβ)-related neural system differences in cognitively normal older men and women ($N = 61$; 41 females, 65–93 years old). We found that men and women showed different associations between Aβ load and hippocampal functional connectivity. During associative memory encoding, in men greater Aβ burden was accompanied by greater hippocampus-prefrontal connectivity (i.e., more synchronized activities), whereas in women hippocampal connectivity did not vary by Aβ burden. For resting-state data, the interaction of gender × Aβ on hippocampal connectivity did not survive multiple comparison in the whole-brain analyses. In the region of interest–based analyses, resting-state hippocampal-prefrontal connectivity was positively correlated with Aβ load in men and was negatively correlated with Aβ load in women. The observed Aβ-related neural differences may explain the accelerated trajectory of cognitive decline and AD progression in women.

1. Introduction

Beta-Amyloid (Aβ) plaques are 1 of the key pathological hallmarks of Alzheimer's disease (AD). The accumulation of Aβ in the brain starts very early in the cascade of AD, and there is a prolonged delay, approximately 10–20 years, until the onset of clinical dementia (Jack et al., 2010; Perrin et al., 2009; Sperling et al., 2011). Consistent with this, Aβ plaque pathology is frequently observed in the brains of older adults without cognitive impairment at autopsy (Bennett et al., 2006) or in vivo using positron emission tomography (PET) amyloid imaging (Aizenstein et al., 2008; Mintun et al., 2006).

Much research has focused on processes that allow elderly adults to maintain normal cognition despite Aβ plaques. Studies have demonstrated that brain activation and functional connectivity are associated with brain Aβ burden in cognitively unimpaired older adults. During episodic memory, increased brain activation in task-positive regions (Edelman et al., 2017; Elman et al., 2014; Mormino et al., 2012; Oh and Jagust, 2013; Vannini et al., 2012) and reduced deactivation in task-negative regions (e.g., default mode network [DMN]) (Huijbers et al., 2014; Sperling et al., 2009; Vannini et al., 2012) were associated with elevated Aβ burden. At rest, both increased (Lim et al., 2014; Mormino et al., 2011) and decreased (Hedden et al., 2009; Huijbers et al., 2014; Mormino et al., 2011; Sheline et al., 2010) functional connectivities in the DMN were found with increased Aβ burden. Furthermore, most recent studies suggested nonlinear relationships between brain activation during spatial distance judgment and

---

[*] Corresponding author at: Charles F. Reynolds III and Ellen G. Detlefsen Endowed Chair of Geriatric Psychiatry, Professor, Department of Psychiatry, Associate Professor, Department of Bioengineering, Associate Professor of Clinical and Translational Science, University of Pittsburgh Clinical and Translational Science, Institute University of Pittsburgh, Pittsburgh, PA, USA. Tel.: +412-246-5464; fax: 412-586-9111.

E-mail address: aizen@pitt.edu (H.J. Aizenstein).

0197-4580/$ – see front matter © 2018 Elsevier Inc. All rights reserved.
https://doi.org/10.1016/j.neurobiolaging.2018.11.020

brain Aβ burden (Foster et al., 2018) and between resting-state functional connectivity and brain Aβ burden (Schultz et al., 2017).

Gender is an important factor associated with AD risk and progression. Compared to men, women are disproportionally affected by AD (Carolyn, 2016) and two-thirds of individuals living with AD are women (Hebert et al., 2013; Alzheimer's Association, 2017). Although men may have a greater risk of mild cognitive impairment (MCI) (Petersen et al., 2010; Roberts et al., 2012), women with MCI deteriorate in cognition almost twice as fast as men with MCI (Holland et al., 2013; Lin et al., 2015; Mielke et al., 2014), suggesting a faster rate of disease progression in women versus men. In addition, genetic studies have shown that the apolipoprotein E (APOE) ε4 variant confers greater risk effects on women relative to men (Bretsky et al., 1999; Farrer et al., 1997; Payami et al., 1994; Poirier et al., 1993).

Neurobiological factors underlying gender differences in AD remain unclear. The present study investigates whether there are gender differences in the association between brain Aβ burden and hippocampal functional connectivity (gender x Aβ) during associative encoding and at resting state in older adults without cognitive impairment. Given gender differences in the prevalence, incidence, and progression of AD, we hypothesized that cognitively normal older men and women would show different Aβ-related alterations in hippocampal functional connectivity. We also hypothesized that these gender differences in relation between Aβ load and hippocampal functional connectivity would be greater in the context of a challenging associative memory task and would persist at resting state but with a moderate effect size.

2. Methods

2.1. Participants

Sixty-one cognitively normal older adults were included in this study. Participants were between the ages of 65 and 93 years (mean ± standard deviation: 75.8 ± 6.4) and 41 (67.2%) were female. Inclusion criteria included age of 65 years or older, fluency in English, and a minimum of 12 years of education. Exclusion criteria included (1) diagnosis of MCI or dementia; (2) history of a major psychiatric or neurological condition; (3) an unstable medical condition that could affect cognition; (4) visual, auditory, or motor deficits sufficient to impair ability to perform the tests; (5) medications affecting cognitive performance; and (6) magnetic resonance (MR)-related contraindications: presence of any metallic implant, claustrophobia, pregnancy, or excessive weight. All participants were evaluated in multiple cognitive domains including memory, visuospatial construction, language, and attention and executive functions to ensure cognitive normality using a comprehensive neuropsychological testing battery nearly identical to that used by the University of Pittsburgh Alzheimer Disease Research Center. Detailed descriptions of the testing battery and diagnostic criteria for MCI or dementia were previously described (Edelman et al., 2017). Individuals who met the criteria for MCI or dementia were excluded from this study. See Table 1 for summarized demographic and clinical characteristics and Table 2 for summarized neuropsychological scores of the sample by gender and amyloid load groups [PiB(+) and PiB(−)] (Pittsburgh compound-B). The Human Use Subcommittee of the Radioactive Drug Research Committees and the institutional review board of the University of Pittsburgh approved all studies. The collected data were previously reported in Edelman et al. (Edelman et al., 2017), which focused on brain activation changes in preclinical AD, and in Nebes et al. (Nebes et al., 2013), which focused on the effects of amyloid burden, white matter hyperintensities, and normal aging on cognitive performance, but neither examined the effects of gender and amyloid burden on hippocampal functional connectivity.

Table 1
Demographic variables and clinical characteristics by gender (N = 61[a])

Characteristic	Group; mean (SD)			
	Female, n = 41	Male, n = 20	Statistical test	*p* value
Age, year[b]	75.5 (6.4)	76.5 (6.6)	$F_{1,59} = 0.32$	0.58
Education, year	14.3 (2.4)	15.3 (2.3)	$F_{1,59} = 2.37$	0.13
Race composition, n (%)			$X^2 = 1.09$	0.58
White	33 (80.5)	18 (90.0)		
Black	7 (17.1)	2 (10.0)		
Asian	1 (2.4)	0(0.0)		
APOE genotype, n (%)[c]			$X^1 = 7.49$	0.01
ε2/ε3	4 (9.8)	3 (15.0)		
ε3/ε3	24 (58.5)	4 (20.0)		
ε3/ε4	3 (7.3)	5 (25.0)		
ε4/ε4	0 (0.0)	1 (5.0)		
Global PiB SUVR	1.58 (0.40)	1.57 (0.29)	$F_{1,59} = 0.01$	0.92
PiB(+), n (%)	8 (19.5)	6 (30.0)	$X^1 = 0.84$	0.36
MMSE score[d]	28.7 (1.4)	28.8 (1.4)	$F_{1,58} = 0.07$	0.80

Key: APOE, apolipoprotein E; MMSE, Mini–Mental State Examination; PiB, Pittsburgh compound-B; SUVR, standardized uptake value ratio.

[a] Unless otherwise indicated.

[b] Age range 65–93 y.

[c] APOE genotyping was available on 44 of 61 participants (31 females and 13 males).

[d] MMSE score (Mini–Mental State Examination) was available on 60 of 61 participants (40 females, 20 males).

2.2. Image acquisition and processing

2.2.1. PiB PET imaging

$[^{11}C]$PiB was synthesized by a simplified radiosynthetic method based on the captive solvent method (Wilson et al., 2000). Fifteen mCi of $[^{11}C]$PiB with high-specific activity (∼2.1 Ci/μmol at end of synthesis) was injected intravenously over 20 seconds. A 20-min PiB PET scanning was performed (4 × 300-second frames) beginning 50 minutes after the $[^{11}C]$PiB injection. The PET scanning was conducted using a Siemens/CTI ECAT HR+ scanner (Siemens Medical Solutions, Knoxville, TN) in 3D imaging mode: 63 axial slices, slice thickness = 2.4 mm, field of view (FOV) = 15.2 cm, intrinsic in-plane resolution = 4.1 mm full-width at half-maximum at FOV center. The scanner is equipped with a neuro-insert to reduce the contribution of scattered photons. PET emission data were reconstructed using filtered back projection with corrections for attenuation, scatter, and radionuclide decay.

2.2.2. MRI acquisition

All MR scanning was performed on a 3T Siemens Trio scanner with 12-channel head coil at the University of Pittsburgh Magnetic Resonance Research Center. Whole-brain functional MR (fMRI) data were acquired axially using gradient-echo echo-planar imaging sequence with the following parameters: repetition time (TR) = 2 seconds, echo time (TE) = 32 ms, flip angle = 90°, FOV = 256 × 256 mm^2, acquisition matrix 128 × 128, slice thickness/gap = 4/0 mm (voxel size = 2 × 2 × 4 mm^3), 28 axial slices. T1-weighted structural images were acquired in the axial plane using a magnetization-prepared rapid gradient echo sequence (T1w MPRAGE) with the following parameters: TR = 2 ms, TE = 3.4 ms, flip angle = 9°, FOV = 240 × 256 mm^2, matrix = 240 × 256, slice thickness/gap = 1/0 mm (voxel size = 1 × 1 × 1 mm^3), 160 slices and generalized autocalibrating partially parallel acquisitions (GRAPPA) acceleration factor = 2. T1w MPRAGE images were used

Table 2
Neuropsychological test performance by gender and PIB status

Characteristics, mean (SD)*	Female (n = 41)		Male (n = 20)		Main and interaction effects		
	PiB(+) (8)	PiB(−) (33)	PiB(+) (6)	PiB(−) (14)	Gender	PiB	Gender × PiB
Memory							
Word List Learning trials	22.0 (4.3)	22.1(3.1)	19.2(3.7)	19.6(3.2)	$F_{1,55} = 5.70$, $p = 0.02$	$F_{1,55} = 0.05$, $p = 0.82$	$F_{1,55} = 0.03$, $p = 0.86$
Word List Learning delayed recall	7.1(2.5)	7.7(1.8)	7.0(2.1)	6.4(2.5)	$F_{1,55} = 1.17$, $p = 0.28$	$F_{1,55} = 0.001$, $p = 0.97$	$F_{1,55} = 0.81$, $p = 0.37$
Rey figure (max = 24)							
Immediate recall	16.1(2.7)	16.1(3.7)	17.8(2.5)	16.6(2.4)	$F_{1,56} = 1.41$, $p = 0.24$	$F_{1,56} = 0.35$, $p = 0.56$	$F_{1,55} = 0.41$, $p = 0.53$
Delayed recall	14.8(2.8)	16.2(3.7)	17.5(2.5)	16.3(2.1)	$F_{1,56} = 2.07$, $p = 0.16$	$F_{1,56} = 0.02$, $p = 0.89$	$F_{1,56} = 1.52$, $p = 0.22$
Logical Memory Story							
A immediate recall	15.0(4.4)	16.5(3.8)	15.2(3.7)	15.2(2.7)	$F_{1,55} = 0.19$, $p = 0.66$	$F_{1,55} = 0.38$, $p = 0.54$	$F_{1,55} = 0.37$, $p = 0.55$
Delay recall	14.5(6.5)	15.1(4.3)	14.4(3.8)	15.2(2.6)	$F_{1,55} < 0.001$, $p = 0.99$	$F_{1,55} = 0.24$, $p = 0.62$	$F_{1,55} = 0.01$, $p = 0.93$
Visuospatial construction							
Block design (max = 24)	14.5(4.6)	13.6(3.6)	17.2(5.5)	13.9(3.6)	$F_{1,56} = 1.49$, $p = 0.23$	$F_{1,56} = 2.8$, $p = 0.10$	$F_{1,56} = 0.85$, $p = 0.36$
Rey figure copy	19.0(2.9)	19.8(2.4)	20.1(1.5)	19.3(1.4)	$F_{1,56} = 0.10$, $p = 0.75$	$F_{1,56} = 0.003$, $p = 0.96$	$F_{1,56} = 1.06$, $p = 0.31$
Language							
Semantic fluency (animals)	19.8(4.7)	20.1(5.8)	21.0(4.3)	21.4(6.4)	$F_{1,56} = 0.49$, $p = 0.49$	$F_{1,56} = 0.04$, $p = 0.85$	$F_{1,56} < 0.001$, $p = 0.99$
Letter fluency (FAS)	48.1(14.9)	44.1(14.7)	45.2(19.2)	39.0.1(9.4)	$F_{1,56} = 0.82$, $p = 0.37$	$F_{1,56} = 1.32$, $p = 0.26$	$F_{1,56} = 0.06$, $p = 0.81$
Boston Naming Test (max = 30)	29.0(1.7)	29.5(0.9)	29.8(0.4)	29.7(0.6)	$F_{1,56} = 4.45$, $p = 0.04$	$F_{1,56} = 0.05$, $p = 0.83$	$F_{1,56} = 0.36$, $p = 0.55$
Attention and executive							
Trail Making Part A (sec)	31.8(9.4)	29.3 (9.1)	27.8(10.9)	32.7(14.5)	$F_{1,56} = 0.01$, $p = 0.94$	$F_{1,56} = 0.12$, $p = 0.73$	$F_{1,56} = 1.18$, $p = 0.28$
Trail Making Part B (sec)	113.7(61.9)	71.9(20.6)	92.6(3.3)	77.5(25.4)	$F_{1,56} = 0.60$, $p = 0.44$	$F_{1,56} = 8.11$, $p = 0.006$	$F_{1,56} = 1.80$, $p = 0.19$
Digit Symbol	44.1(17.2)	55.1(10.9)	47.3(12.7)	48.4(9.3)	$F_{1,56} = 0.22$, $p = 0.65$	$F_{1,56} = 2.66$, $p = 0.11$	$F_{1,56} = 1.78$, $p = 0.19$
Stroop color-word	33.0(15.5)	40.5(8.9)	30.2 (5.2)	32.8(8.3)	$F_{1,54} = 2.72$, $p = 0.11$	$F_{1,54} = 2.50$, $p = 0.12$	$F_{1,54} = 0.59$, $p = 0.45$
Clock drawing (max = 15)	14.8(0.5)	14.2(0.8)	14.7 (0.5)	14.2(0.9)	$F_{1,56} = 0.01$, $p = 0.91$	$F_{1,56} = 4.29$, $p = 0.04$	$F_{1,56} = 0.05$, $p = 0.82$
Face/Name Recognition %	70.0(9.3)	71.0(11.2)	65.5 (11.3)	61.0(12.4)	$F_{1,57} = 2.19$, $p = 0.14$	$F_{1,57} = 0.004$, $p = 0.95$	$F_{1,57} = 1.84$, $p = 0.18$

to facilitate and improve the normalization of fMRI data into the Montreal Neurological Institute (MNI) template space. Resting-state fMRI data (5 minutes) were collected, and participants were instructed to fixate on a central crosshair and to stay awake during image acquisition. Task fMRI data were collected while participants were performing a face-name memory associative memory task. The face-name memory encoding task is a mixed block/event-related design task. Each run of the task lasted 4 minutes 36 seconds, consisting of 2 experimental blocks and 2 control blocks, interspersed with 25-sec fixation. Each block lasted 48 seconds, containing 8 sequential trails of face-name pairs, 5 seconds each trial with 1-second intertrial interval. During the experimental blocks, participants were presented novel face-name pairs and were asked to subjectively decide and respond with an MR-compatible glove whether or not each name was a good fit for the face. This subjective decision was designed to strengthen the associative encoding of the face-name pairs (Sperling et al., 2003a). For the control blocks, 2 familiar face-name pairs, 1 female face-name pair, and 1 male face-name pair were repeatedly presented to the participants. The participants were trained and thus familiar with these 2 face-name pairs in the pre-scan session. Of the 61 participants, 44 participants completed 3 runs of the face-name task, 11 completed 2 runs, and 4 completed 1 run.

2.2.3. *PET data processing*

The dynamic [11C]PiB acquisition frames are inspected for evidence of interframe motion. If suspected, the automated image registration algorithm with parameters optimized for PET to PET registration is applied to the dynamic [11C]PiB images on a framewise basis to correct for interframe motion (Woods et al., 1993). A summed PET image is then generated over the 50- to 70-minute postinjection interval. The structural T1w MPRAGE MR image was reoriented such that the axial image planes are parallel to the plane intersecting both the anterior and posterior cerebral commissure (AC-PC). The AC-PC aligned MPRAGE MR image was then coregistered with the summed [^{11}C]PiB image using the automated image registration algorithm (PET-MR) (Woods et al., 1993). The resulting PET-MR spatial transformation was applied to the summed [^{11}C]PiB image, which was resliced into the AC-PC-aligned MPRAGE image space.

A set of volumes of interests (VOIs), as previously defined(Cohen et al., 2009), were separately hand-drawn on the AC-PC-aligned MPRAGE MR image, which include frontal cortex (FRC; ventral and dorsal), anterior cingulate gyrus (ACG: subgenual and pregenual), anteroventral striatum (AVS), mesial temporal cortex (includes hippocampus and amygdala), precuneus/posterior cingulate cortex (PRC; ventral, middle, and dorsal thirds), parietal cortex (PAR), lateral temporal cortex (LTC), occipital cortex (OCC; calcarine and pole), and cerebellum. These hand-drawn VOIs are used to sample the resliced [^{11}C]PiB image, and regional radioactivity concentrations were calculated and converted into units of standardized uptake value (SUV) using the injected dose of [^{11}C]PIB and the subject's body mass. The unitless SUV outcome is normalized to nonspecific uptake (cerebellum), yielding an SUV ratio (SUVR) measure that compares favorably to fully quantitative measures of specific radiotracer retention (Lopresti et al., 2005). Regional SUVR outcomes were partial volume corrected using a previously validated method that corrects for the dilution of PET signal attributable to the limited spatial resolution of the PET scanner (Meltzer et al., 1996, 1998, 2000; Lopresti et al., 2005; Price et al., 2005). This method includes a two-component approach that corrects PET data for the dilutional effect of expanded cerebrospinal fluid spaces accompanying normal aging and disease-related cerebral atrophy using the FSL software (University of Oxford, Oxford, UK). A global PiB retention index reflecting cerebral amyloid load is computed from the SUVR values from the 6 most relevant VOIs (ACG, FRC, LTC, PAR, PRC, and AVS). Participants were classified as PiB positive or negative [PiB(+) or PiB(−)] by using a sparse k-means cluster analysis (Cohen et al., 2013).

2.3. Functional MRI data preprocessing

Functional images were preprocessed in SPM12 (Wellcome Trust Centre for Neuroimaging, http://www.fil.ion.ucl.ac.uk/spm/) implemented in Matlab 2015 (MathWorks, Natick, MA) for slice timing correction, motion correction, coregistration, image normalization, resampling at a $2 \times 2 \times 2$ mm^3 voxel size, and 8-mm gaussian smoothing. The mean functional image was coregistered to individual T1w MPRAGE structural image using an affine registration (mean functional image -> T1 MPRAGE image). The T1w MPRAGE structural image was manually skull-stripped in ITK-SNAP, segmented, and warped into the MNI common template space using SPM's unified segmentation/normalization procedure (T1 MPRAGE image->MNI template). After slice timing correction (the temporally middle slice as the reference), the functional data were realigned to the mean functional image using the two-pass rigid-body realignment procedure for motion correction, which were further resliced and normalized into the MNI common space using the functional-structural coregistration matrix (mean functional image -> T1 MPRAGE image) and the structural-MNI deformation field (T1 MPRAGE image->MNI template). Furthermore, for resting-state fMRI data, motion artifacts were removed using the wavelet despike method (Patel et al., 2014), and nuisance signals from the white matter, cerebrospinal fluid, and residual motion effect were regressed out in a multiple linear regression with regressors of no interest including principal time series from the white matter and cerebrospinal fluid and 6 motion parameters. The residual resting-state fMRI data were then temporally band-pass filtered (a second-order Butterworth bandpass filter) with the frequency range of 0.008–0.15 Hz to extract the low-frequency resting-state blood oxygen-level dependent signal.

2.4. Functional connectivity

Both task-based and resting-state connectivity of the hippocampus were examined in this study. Two seed regions, left and right hippocampus, were created with the anatomically defined automated anatomical labeling atlas (Tzourio-Mazoyer et al., 2002) using the WFU Pick-Atlas tool. For task-based connectivity, generalized psychophysiological interaction (gPPI) analysis (Cisler et al., 2014; Friston et al., 1997; McLaren et al., 2012) was performed to estimate functional connectivity between hippocampus and voxels in the brain. Principal time series (i.e., the eigenvariate) was generated for each seed region, left and right hippocampus, using singular value decomposition (implemented in Matlab 2015) from hippocampal fMRI data during the face-name task. Although differences are subtle, compared to using average time series, principal component analysis (PCA)–based method can identify the primary blood oxygen-level dependent time series (Carbonell et al., 2012; Zhou et al., 2009) and is robust to inclusion of voxels that do not follow the primary time series of the region. This is, particularly, relevant for brain regions defined anatomically, such as the whole hippocampus. Because the anatomic definition includes diverse voxels, which have different functional patterns, it is appropriate to weight the voxels accordingly using PCA. This approach generates a time series more representative of the principal signal and minimizes the contribution of irrelevant voxels. Principal time series of the seed region (left or right hippocampus), task conditions (novel face-name pairs, familiar repeated face-name pairs), interaction variables (seed times series × task condition), and motion parameters were included in the design matrix. PPI connectivity maps (left or right hippocampus) during associative encoding (i.e., novel face-name pairs vs. repeated familiar face-name pairs), during novel blocks (novel face-name pairs vs. fixation), and during repeated blocks (repeated familiar face-name pairs vs. fixation) were computed for each participant.

Resting-state hippocampal connectivity was estimated using a seed-based correlation analysis. Similarly, using singular value decomposition, principal time series of the resting-state data was computed from left or right hippocampus. Resting-state connectivity between the seed region (left or right hippocampus) and a given voxel was calculated as the correlation between the seed principal time series and the voxel time series. For each participant, correlation was calculated voxelwise within the brain, generating functional connectivity or correlation coefficient maps of left and right hippocampus, respectively. The connectivity or correlation maps were converted into Z-score maps via Fisher's r-to-z transformation.

2.5. Second-level analyses

Task-based hippocampal functional connectivity maps (left or right hippocampal gPPI maps) were entered into a statistical nonparametric mapping method (SnPM, http://warwick.ac.uk/snpm) to test the effects of gender, Aβ load, and the interaction of gender × Aβ on hippocampal connectivity during associative memory encoding. SnPM uses the general linear model to construct pseudo t-statistic images and uses permutation testing to compute nonparametric p-values, control for multiple comparisons, and assess significance (Nichols and Holmes, 2002, 2004). To test if the association between connectivity and Aβ varies by gender, a linear regression model was used with main effects of gender and Aβ, as well as the interaction of gender × Aβ. In these tests, Aβ burden was treated as a continuous variable (PiB SUVR). To control for nonparametric multiple comparisons, a permutation-based method was used in SnPM with 5000 permutations and a whole-brain intracranial volume mask. The intracranial volume mask has a total volume of 1,885,673 mm^3 (558,718 voxels, $1.5 \times 1.5 \times 1.5$ mm^3). An initial cluster-forming threshold of $p < 0.001$ was used, and clusters with an extend threshold of $p < 0.05$ familywise errors were considered to be significant. These effects were further tested, controlling for age, education, and number of runs for the fMRI task.

Sensitivity analysis was performed to test the robustness of the results with a subset of the original sample, excluding those with extreme values of Aβ burden or functional connectivity. Subjects with extreme values of Aβ burden were identified with the Tukey Method (1.5 × interquartile range) (Hoaglin et al., 2012) in SPSS (SPSS 24.0 version, Chicago, IL, USA). Regression outliers of functional connectivity and Aβ burden were identified with Cook's distance ($D > 0.5$) in SPSS (Cook, 1977).

For post hoc analyses, a region of interest (ROI) mask was created from prefrontal regions that showed significant gender x Aβ interactions. Task-based connectivity between the left or right hippocampus and the corresponding prefrontal ROI mask was extracted. To dissect the direction of the interaction and the magnitude of the effect size, Pearson correlation was performed in SPSS to examine the linear relationships between functional connectivity and Aβ load stratified by gender. To explore whether the observed interaction on novel-repeated blocks were driven by novel blocks or by repeated blocks, hippocampal functional connectivities during novel blocks (novel face-name pairs–fixation) and during repeated blocks (repeated familiar face-name pairs–fixation) were also extracted from above prefrontal ROIs.

For resting-state data, both voxelwise and ROI-based analyses were performed to evaluate the effects of gender and Aβ on hippocampal connectivity. In the voxelwise analyses, similar to task-based data, resting-state hippocampal (left or right) connectivity maps were entered into SnPM to evaluate the effects of gender, Aβ load, and the interaction of gender x Aβ. In the post hoc ROI-based analyses, resting-state connectivity between hippocampus and the prefrontal ROIs (from gender × Aβ interactions on task-based connectivity) was extracted and Pearson correlation was then performed to examine the associations between resting-state connectivity and Aβ load stratified by gender.

Analyses of variances were performed in SPSS to examine the effects of gender, PiB status [PiB(+) and PiB(−)], and the interaction of gender x PiB status on neurocognitive data. In addition to classifying Aβ levels categorically [PiB(+) and PiB(−)], Aβ load was also modeled as a continuous variable (PiB SUVR). Pearson correlation analyses were performed in SPSS to assess the linear associations between PiB SUVR and neurocognitive performances. We also tested these effects controlling for age, education, and/or ApoE status.

3. Results

3.1. Participant characteristics

Demographics, clinical characteristics, and neurocognitive data are presented in Tables 1 and 2. Males and females did not significantly differ on age, education, race, global PiB SUVR, PiB(+)%, or Mini–Mental State Examination scores. Of 61 participants, APOE genotype results were available on 44 participants (31 women and 13 men). In this sample, more men had at least 1 ApoE4 allele ($n = 6$) than did women ($n = 3$) ($p = 0.01$, Fisher's exact test).

3.2. Neurocognitive outcomes

There were no gender differences in memory, visuospatial construction, language and attention, or executive domains (see Table 2). However, women performed significantly better on word-list learning and Stroop color-word interference and marginally better on word-list delayed recall tests than men. Conversely, men performed slightly better than women on Boston Naming Test. There was no significant main effect of PiB status on neurocognitive measures of memory, visuospatial construction, or language domains. There were no gender × PiB interactions in relation to neurocognitive outcomes. Subsequent face-name recognition accuracy was also measured, and there was no significant main effect of gender, PiB status, or gender × PiB interaction on subsequent face-name recognition accuracy (Table 2).

PiB(+) participants performed significantly worse than PiB(−) participants in attention and executive subtests including the trail making part B. PiB(+) participants performed better than PiB(−) participants in clock drawing. PiB status remained significantly or of a trend toward significance associated with trail making part B and clock drawing scores when controlling for age and education [trail making part B: $F(1,54) = 6.56$, $p = 0.01$, clock drawing: $F(1,54) = 5.70$, $p = 0.02$], as well as additionally ApoE status [a subset of 43 subjects had ApoE status, trail making part B: $F(1,36) = 4.77$, $p = 0.04$, clock drawing: $F(1,36) = 3.38$, $p = 0.07$]. When Aβ load was modeled as a continuous variable (PiB SUVR), controlling for gender, PiB SUVR was positively associated with trail making part B score [$r(57) = 0.30$, $p = 0.02$, 95% confidence interval (CI) = 0.17, 0.48] and negatively associated with digital symbol substitution score [$r(57) = -0.29$, $p = 0.02$, 95% CI = −0.50, −0.06] and Stroop color-word interference [$r(55) = -0.33$, $p = 0.01$, 95% CI = −0.54, −0.05] scores. PiB SUVR showed a trend toward a significant correlation with trail making part B [$r(55) = 0.23$, $p = 0.09$, 95% CI = 0.08, 0.41], digital symbol substitution score [$r(55) = -0.22$, $p = 0.10$, 95% CI = −0.43, −0.01], and Stroop color-word interference [$r(53) = -0.28$, $p = 0.04$, 95% CI = −0.50, −0.02] when controlling for gender, age, and education. PiB SUVR remained marginally significantly correlated with trail making part B [$r(37) = 0.29$, $p = 0.07$, 95% CI = 0.11, 0.52] but not with digital symbol substitution score or Stroop color-word interference (p's > 0.13, $n = 43$) when controlling for gender, age, education, and ApoE within a subset of the subjects.

3.3. Functional connectivity

Table 3 and Fig. 1A present the main and interaction effects of gender and Aβ load on hippocampal connectivity during associative encoding (corrected $p < 0.05$). There were no significant main effects of gender or Aβ load on hippocampal functional connectivity. Gender × Aβ interactions were observed for both left and right hippocampal connectivity with prefrontal regions encompassing medial prefrontal cortex, anterior cingulate, left superior frontal gyrus, and left middle frontal gyrus. A gender × Aβ interaction was also observed for right hippocampal connectivity with left occipital gyrus. The gender × Aβ interaction for hippocampal connectivity persisted when controlling for age, education, and number of runs for the fMRI task.

Scatterplots in Fig. 1B visualize the gender × Aβ interactions on task-based functional connectivity between hippocampus and prefrontal regions. Specifically, hippocampal-prefrontal connectivity was positively correlated with Aβ load in men [left hippocampal connectivity: $r(18) = 0.70$, $p = 0.001$, 95% CI = 0.53, 0.92 and right hippocampal connectivity: $r(18) = 0.65$, $p = 0.002$, 95% CI = 0.43, 0.86] but not in women [left hippocampal connectivity: $r(39) = 0.01$, $p = 0.95$, 95% CI = −0.35, 0.27, and right hippocampal connectivity: $r(39) = 0.06$, $p = 0.71$, 95% CI = −0.48, 0.27]. There are no significant associations between functional connectivity and

Table 3

Gender-by-Aβ load ANOVAs of hippocampal functional connectivity during the face-name associative memory task (corrected $p < 0.05$)

Gender-by-Aβ ANOVA	Brain region	Brodmann area (BA)	Peak MNI coordinates (x,y,z)	t-score	Size (mm^3)
Left hippocampal functional connectivity					
Main effect of gender	None				
Main effect of Aβ	None				
Gender by Aβ interaction	mPFC/ACC, L SFG, L MFG	BA 10, 32, 24	−4, 50, 8	4.21	3192
Right hippocampal functional connectivity					
Main effect of gender	None				
Main effect of Aβ	None				
Gender by Aβ interaction	mPFC/ACC, L SFG, L MFC	BA 10	−22, 54, -2	5.34	1592
	L MCG/Cuneus	BA 17, 18, 19, 39	−26, -82, 8	4.47	1352

Key: ACC, anterior cingulate cortex; ANOVA, analyses of variance; L, left; mPFC, medial prefrontal cortex; MCG, middle occipital gyrus; MFG, middle frontal gyrus; MNI, Montreal Neurologic Institute; SFG, superior frontal gyrus.

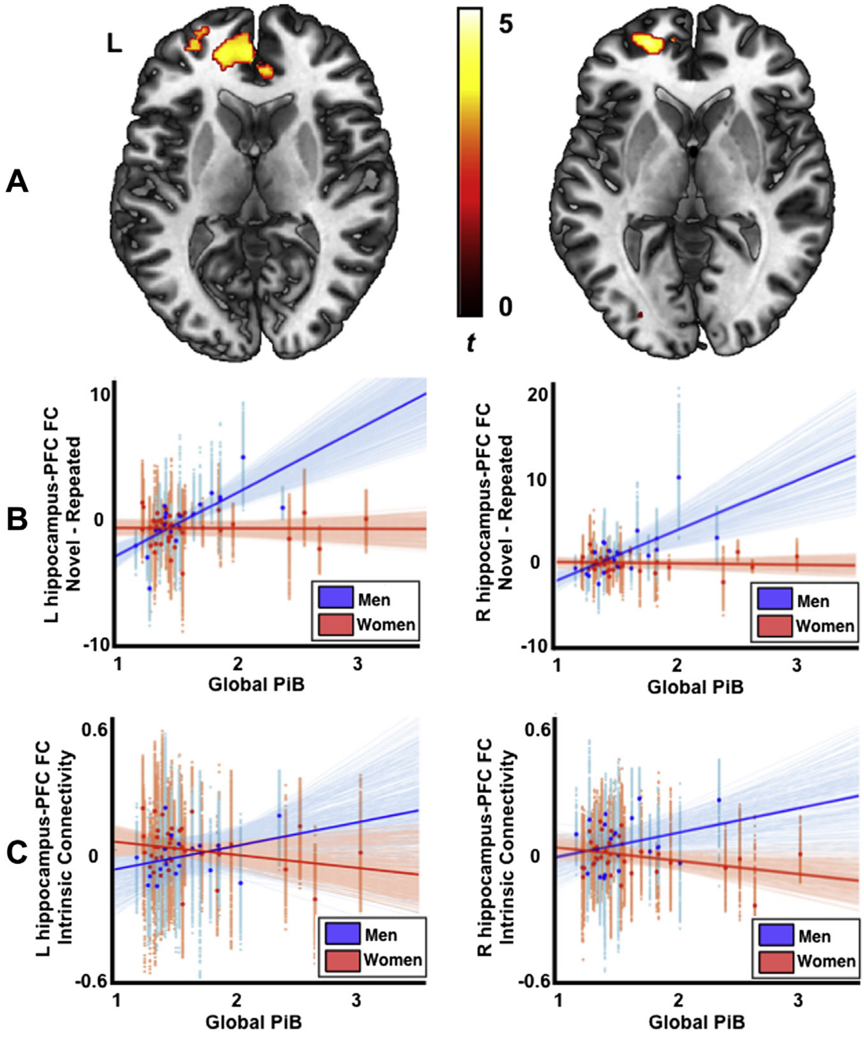

Fig. 1. There are significant gender differences in the associations between brain amyloid (Aβ) load and hippocampal functional connectivity. Brain Aβ load was measured as a global PiB retention index computed from the SUVR values from the 6 most relevant brain regions. (A) Gender × Aβ interactions on left and right hippocampal functional connectivity during associative encoding (left panel: left hippocampal connectivity, right panel: right hippocampus connectivity). Hippocampal functional connectivities during associative encoding and during resting state were voxelwise extracted from prefrontal regions identified in A. The extracted functional connectivities (beta weights) were voxelwise plotted against Aβ load in B and C (small dots: voxelwise beta estimate, bold dots: median beta estimate across the prefrontal ROI). (B) Scatterplots of Aβ load and hippocampus-prefrontal connectivity during associative encoding (blue: men, red: women). (C) Scatterplots of Aβ load and hippocampus-prefrontal connectivity during resting state (blue: men, red: women). Abbreviations: L, left; R, right; PFC, prefrontal cortex; PiB, Pittsburgh compound-B; ROI, region of interest; SUVR, standardized uptake value ratio. (For interpretation of the references to color in this figure legend, the reader is referred to the Web version of this article.)

subsequent recognition accuracy of the face/name pairs [left hippocampal connectivity: r (59) = −0.06, p = 0.67, and right hippocampal connectivity: r(59) = −0.16, p = 0.22] or between functional connectivity and cognitive measures (uncorrected p's > 0.05). Furthermore, the observed interaction on hippocampal connectivity were driven by both novel and repeated blocks, with a greater functional connectivity during novel blocks and a lower functional connectivity during repeated blocks in PiB+ men than in PiB+ women, as shown in Supplementary Fig. 3.

We did not observe significant main effects of gender and Aβ load on resting-state functional connectivity in the voxelwise analyses. The interaction effect of gender × Aβ on resting-state hippocampal connectivity did not survive multiple comparison either (e.g., left hippocampus: left superior frontal gyrus/medial frontal gyrus [BA 10, 32], peak t = 3.63, peak xyz: [−20, 48, 6], cluster size: 552 mm^3, uncorrected $p < 0.005$). Prefrontal ROIs from the gender × Aβ interactions on task-based connectivity (in Fig. 1A) were used to extract resting-state connectivity between hippocampus in the ROI-based post hoc analyses (Fig. 1C). We found significant interaction effects of gender × Aβ [left hippocampus: F(1,54) = 3.60, p = 0.063; right hippocampus: F(1,54) = 4.60, p = 0.037], marginally significant main effects of gender [left hippocampus: F(1,54) = 4.31, p = 0.043; right hippocampus: F(1,54) = 2.91, p = 0.094], and no significant main effects of Aβ (p's > 0.52) on the extracted resting-state connectivity. As shown in Fig. 1C, the extracted resting-state connectivity showed a lower magnitude positive association with Aβ load in men [moderate effect size: left hippocampal connectivity: r(18) = 0.32, p = 0.17, 95% CI = −0.25, 0.77; right hippocampal connectivity: r(18) = 0.28, p = 0.23, 95% CI = −0.22, 0.62], whereas resting-state connectivity was negatively correlated with Aβ load in women [moderate effect size: left hippocampal connectivity: r(36) = −0.24, p = 0.15, 95% CI = −0.57, 0.12; right hippocampal connectivity: r(36) = −0.32, p = 0.05, 95% CI = −0.61, 0.01].

In the sensitivity analysis, 6 participants were removed from the original sample based on amyloid load (n = 5, Aβ load >2.06 based on the Tukey's Method) and functional connectivity (n = 1, Cook's Distance D > 0.5), yielding a subset of 55 participants (subset N =

55) (Supplementary Fig. 1). Consistent with the primary analysis, sensitivity analysis showed significant gender × Aβ interactions on both left and right hippocampal connectivities with prefrontal regions during associative memory encoding (Supplementary Fig. 2A, corrected $p < 0.05$). In this subset, hippocampus-prefrontal connectivity was also positively correlated with Aβ load in men [left hippocampal connectivity: r(16) = 0.72, 95% CI = 0.55 0.88; right hippocampal connectivity: r(16) = 0.67, 95% CI = 0.34 0.85] and not in women [left hippocampal connectivity: r(35) = −0.09, 95% CI = −0.37, 0.19; right hippocampal connectivity: r(35) = −0.28, 95% CI = −0.55, 0.14] (Supplementary Fig. 2B). In contrast to moderate effect on resting-state connectivity in the post hoc ROI analyses with the full resting-state sample (N = 58), sensitivity analysis did not find significant association between resting-state hippocampal-prefrontal connectivity and Aβ load in men or women (*p*'s > 0.4).

4. Discussion

This study investigated gender differences in the associations between brain Aβ deposition (i.e., global PiB retention) and hippocampal functional connectivity in cognitively intact older adults. We found men and women have different patterns in hippocampal functional connectivity with increased amyloid burden. Specifically, in men, greater Aβ burden was accompanied by greater functional connectivity between hippocampus and prefrontal regions, whereas in women hippocampal connectivity did not vary by amyloid burden. We found this pattern of associations using voxelwise analyses of hippocampal functional connectivity during a face-name associative memory fMRI task. The effect was significant for both right and left hippocampal connectivities during associative encoding. With prefrontal regions identified from task-based analyses, we performed ROI-based analyses on resting-state fMRI data and found that hippocampal-prefrontal connectivity at rest was positively correlated with Aβ load in men and was negatively correlated with Aβ load in women. However, whole-brain voxelwise analyses of resting-state hippocampal connectivity did not survive multiple comparison.

Gender differences in Aβ-related compensation may relate to different trajectories of steroid hormones, estradiol in particular, with aging between men and women (Farage et al., 2012). In contrast to no significant change of estrogen with advancing age in men, there is a substantial decrease of estrogen, particularly estradiol, in midlife and older women (Farage et al., 2012). Extensive animal studies have revealed the effects of estrogen on the structural and synaptic plasticity of the hippocampus (Foy et al., 2008; Hara et al., 2012; Liu et al., 2008; McEwen, 2002; Morrison et al., 2006; Woolley et al., 1990; Woolley and McEwen, 1993) and the prefrontal cortex (Dumitriu et al., 2010; Hao et al., 2006; Morrison et al., 2006; Rapp et al., 2003; Wang et al., 2010). Human studies have also implicated the effects of estradiol on the memory circuitry (Barth et al., 2016; Duff and Hampson, 2000; Dumas et al., 2010; Grigorova et al., 2006; Shaywitz et al., 1999). In the present study, a data-driven (PCA) method was used to select the hippocampal voxels most associated with encoding during the face-name associative memory task. The particular voxels identified are located in the anterior hippocampus, primarily CA3, which matches the location previously identified with this task using high-resolution MR/fMRI (Zeineh et al., 2003). Although previous findings focused on the effects of estrogen on the synaptic plasticity of hippocampal CA1 subfield (McEwen, 2002; Woolley et al., 1990; Woolley and McEwen, 1993), new studies have extended to the dentate gyrus and CA3 subfield of the hippocampus (Briz et al., 2015; Kim et al., 2006; Zhang et al., 2013). Specifically, long-term estrogen deprivation was found to cause gender-specific hypersensitivity of the CA3 subfield to ischemic stress and to the neurotoxic effects of Aβ_{1-42} in ovariectomized (i.e., surgical menopause) female rats, but not in orchiectomized male rats (Zhang et al., 2013). It is possible that the dramatic drop in estrogen levels during the menopause transition may render this circuitry particularly vulnerable to synaptic plasticity loss and Aβ neurotoxicity in postmenopausal women. Men generate estrogen from testosterone and adrenal androgens and do not experience as dramatic a loss of estrogen with aging. Thus, the estrogen-related neural plasticity loss and hypersensitivity to Aβ-induced damage may be specific for women, which may explain the reduction in fMRI markers of compensation and the faster rate of cognitive decline and AD progression. Although men show no dramatic change in estrogen, they do show a modest gradual decline in testosterone with advancing age (Snyder, 2017). Recent studies have shown the effects of testosterone on hippocampal synaptic plasticity in male rats (Atwi et al., 2016; Schulz and Korz, 2010), and high concentrations of serum testosterone are associated with better cognitive performance in older men (Matsumoto, 2002). Therefore, it is also possible that age-related decline in testosterone concentrations might contribute to cognitive decline in older men.

The effects of hippocampal hyperactivity/hyperconnectivity on cognitive performance and outcome are mixed in the literature. Some studies have shown that hippocampal hyperactivity/hyperconnectivity is beneficial. Greater hippocampal activation was observed during successful associative encoding (Miller et al., 2008) and was significantly related to a better visual memory factor score (Mormino et al., 2012). Greater hippocampal connectivity during associative encoding and during resting state was linked with better memory performance in older adults without cognitive impairment (Lim et al., 2014; Nyberg, 2016; Salami et al., 2014) and in healthy individuals (25–80 years of age) (Nyberg, 2016; Salami et al., 2014). In contrast, others have suggested that hippocampal hyperactivity is deleterious and is associated with quicker cognitive decline (Dickerson et al., 2004; O'Brien et al., 2010). Dickerson et al. reported that greater clinical decline at 2.5-year follow-up was associated with greater extent of activation in the right hippocampus at baseline. Using longitudinal fMRI, O'Brien et al. found that, in older adults without dementia, individuals with more rapid decline at 2-year follow-up had the highest hippocampal activation at baseline and greatest loss of hippocampal activation at 2-year follow-up. Furthermore, treatment studies showed that normalizing hippocampal hyperactivity in patients with MCI have been shown to improve task-related memory performance (Bakker et al., 2012, 2015). In our study, we did not find a significance association between cognitive performance and fMRI connectivity. We suspect this may be because the neural system response (measured by fMRI) reflects a physiologic homeostatic response, which can lead to disparate effects on behavior. For example, hypertension may maintain perfusion and also lead to hypoperfusion. The hippocampal frontal hyperconnectivity observed in preclinical AD may serve a compensatory function and maintain performance in some individuals. It also can be seen as dedifferentiation in-so-far as it may involve engagement of less-specific neural resources.

Many studies have demonstrated the progression of AD from the medial temporal lobe (MTL)/hippocampal hyperactivity/hyperconnectivity at a preclinical stage [in cognitively normal older adults with high Aβ burden (Edelman et al., 2017; Mormino et al., 2012; Oh and Jagust, 2013; Vannini et al., 2012) and in early MCI patients (Celone et al., 2006; Dickerson et al., 2005; Hämäläinen et al., 2007; Pizzi et al., 2018)] to hypoactivity/hypoconnectivity at a later stage of the disease [in late MCI and AD patients (Hämäläinen et al., 2007; Pizzi et al., 2018; Sperling et al., 2003)]; for review, see Sperling (2011). Specifically, with a large sample size (N = 135), Pizzi et al. reported that compared to cognitively unimpaired older adults, non-converter MCI individuals (i.e., did not convert to AD in 24 months) showed MTL/hippocampal hyperconnectivity and converter MCI individuals (i.e., converted to AD in 24 months) showed MTL/hippocampal hypoconnectivity (Pizzi et al., 2018). These evidences collectively suggest the transition of hyperactivity to hypoactivity and connectivity of MTL/hippocampal happens at the late stage of MCI. On the other hand, brain activity and resting-state functional connectivity have been shown to follow a nonlinear (i.e., quadratic) relationship with Aβ SUVR in cognitively unimpaired older adults, suggesting this transition may occur at the preclinical stage of AD (Foster et al., 2018; Schultz et al., 2017). Specifically, Foster et al. found that during a spatial distance judgment task, participants with slightly elevated Aβ showed hyperactivity, whereas those with extremely elevated Aβ showed hypoactivity in bilateral angular/temporal and medial prefrontal cortices (Foster et al., 2018). Schultz et al. reported a similar nonlinear pattern on resting-state connectivity of the default mode and salience networks (interaction effect of Aβ × tau), with increased functional connectivity in Aβ+ participant with a low neocortical tau level and decreased functional connectivity in Aβ+ participants with a high tau level(Schultz et al., 2017). Although in our current sample men and women did not significantly differ on global PiB SUVR ($p = 0.92$) or PiB(+)% ($p = 0.36$), the distribution of global PiB SUVR seemed to be imbalanced (4 women but no men showed extreme PiB SUVR values > 2.06). To address this imbalance, sensitivity analyses were performed with a subset of the sample ($N = 56$) and a narrow range of PiB SUVR (≤ 2.06). Similar gender differences in hippocampal connectivity were found with this subset as with the entire sample in the primary analyses. However, with our current sample, which focuses on cognitively unimpaired older adults, we are unable to test and rule out the possibility of hypoconnectivity with extreme high Aβ load. However, using the same face-name associative encoding task, multiple studies have shown that individuals at the early phase of MCI exhibited MTL hyperactivity (Celone et al., 2006; Dickerson et al., 2005). This suggests that, at least for this task, a sample with a greater range of cognitive impairment (further along in the AD biomarker cascade) may be necessary to demonstrate the nonlinear pattern.

Several limitations of this study should be considered. Sex hormones were not measured, and we were not able to explore how functional connectivity is related to levels of estradiol, testosterone, or other sex steroids. Current medications were recorded, and no participants were on estrogen at the time of the scans. In this study, we did not observe amyloid-related functional connectivity changes in women. It is possible that women showed more subtle changes in hippocampal connectivity that did not survive stringent multiple comparisons. This study has a relatively modest sample size ($N = 61$), which may not have sufficient power to detect these subtle changes. It is also possible that women may have amyloid-related connectivity changes in brain regions other than hippocampus. This study only evaluated hippocampal functional connectivity and thus did not capture such changes in women. A cross-sectional instead of longitudinal design was used in this analysis. The cross-sectional design evaluates Aβ-related differences through correlations, which are inherently vulnerable to intersubject variance and cohort effects. ApoE genotype results were only available on 44 participants (31 women and 13 men), and more men had at least 1 ApoE4 allele ($n = 6$) than did women ($n = 3$) in this study. Using a comprehensive neuropsychological testing battery, participants were evaluated in multiple cognitive domains to ensure cognitive normality. Of these tests, women performed better in the Word List Learning test and men performed better in the Boston Naming Test, which may reflect different patterns of cognitive performance in older men and women. The face-name memory encoding task used in this study is a mixed block/event-related design task. The event-related aspect of this task is not optimized for event-related analyses (not jittered and rapid events). Further block-design in general has been shown to have a greater effect size and is less susceptibility to between-subject variability in the haemodynamic response function, a particular concern in older populations (Huettel et al., 2001). Therefore, in this and previous literature (Edelman et al., 2017; Jahani et al., 2017; Sperling et al., 2003), we and others have focused on the block-design aspect of the task. However, including event-related behavior regressors in the gPPI model could potential address interpretive issues with the task. Future studies with more participants, longitudinal designs, task behavior regressors, hormonal measures, and ApoE genotype data will be important to understand gender differences in amyloid burden, hippocampal functional connectivity, and cognitive performance.

In summary, an Aβ-related increase in hippocampal-prefrontal functional connectivity occurs before memory decline and may be an early marker reflecting a homeostatic response in the memory network. We found that these responses are greater in men than women. We suggest that this finding may explain gender differences in disease trajectories. Longitudinal studies are required to confirm this finding. Nonetheless, characterizing gender differences in responses for AD-related pathologies, as in the present study, can help guide the development of gender-specific prevention and treatment strategies.

Disclosure

The authors and their institutes have no financial interests to disclose in this work.

Acknowledgements

This work was supported by National Institute of Aging, National Institutes of Health (NIH) grants RF1 AG025516 to WEK and HJA, AG030653 and AG041718 to MIK, and by National Heart Lung and Blood Institute, NIH, grant K24-123565 to RCT. The content is solely the responsibility of the authors and does not necessarily represent the official views of the NIH.

Appendix A. Supplementary data

Supplementary data to this article can be found online at https://doi.org/10.1016/j.neurobiolaging.2018.11.020.

References

Aizenstein, H.J., Nebes, R.D., Saxton, J.A., Price, J.C., Mathis, C.A., Tsopelas, N.D., Ziolko, S.K., James, J.A., Snitz, B.E., Houck, P.R., Bi, W., Cohen, A.D., Lopresti, B.J., DeKosky, S.T., Halligan, E.M., Klunk, W.E., 2008. Frequent amyloid deposition without significant cognitive impairment among the elderly. Arch. Neurol. 65, 1509.

Alzheimer's Association, 2017. Alzheimer's disease facts and figures. Alzheimer's Dement. 13, 325–373.

Atwi, S., McMahon, D., Scharfman, H., MacLusky, N.J., 2016. androgen modulation of hippocampal structure and function. Neuroscientist 22, 46–60.

Bakker, A., Krauss, G.L., Albert, M.S., Speck, C.L., Jones, L.R., Stark, C.E., Yassa, M.A., Bassett, S.S., Shelton, A.L., Gallagher, M., 2012. Reduction of hippocampal hyperactivity improves cognition in amnestic mild cognitive impairment. Neuron 74, 467–474.

Bakker, A., Albert, M.S., Krauss, G., Speck, C.L., Gallagher, M., 2015. Response of the medial temporal lobe network in amnestic mild cognitive impairment to therapeutic intervention assessed by fMRI and memory task performance. NeuroImage Clin. 7, 688–698.

Barth, C., Steele, C.J., Mueller, K., Rekkas, V.P., Arélin, K., Pampel, A., Burmann, I., Kratzsch, J., Villringer, A., Sacher, J., 2016. In-vivo dynamics of the human Hippocampus across the menstrual cycle. Scientific Rep. 6, 584.

Bennett, D.A., Schneider, J.A., Arvanitakis, Z., Kelly, J.F., Aggarwal, N.T., Shah, R.C., Wilson, R.S., 2006. Neuropathology of older persons without cognitive impairment from two community-based studies. Neurology 66, 1837–1844.

Bretsky, P.M., Buckwalter, J.G., Seeman, T.E., Miller, C.A., Poirier, J., Schellenberg, G.D., Finch, C.E., Henderson, V.W., 1999. Evidence for an interaction between apolipoprotein E genotype, gender, and Alzheimer disease. Alzheimer Dis. Assoc Disord. 13, 216.

Briz, V., Liu, Y., Zhu, G., Bi, X., Baudry, M., 2015. A novel form of synaptic plasticity in field CA3 of hippocampus requires GPER1 activation and BDNF release. J. Cell Biol. 210, 1225–1237.

Carbonell, F., Bellec, P., Shmuel, A., 2012. Global and system-specific resting-state fMRI fluctuations are uncorrelated: principal component analysis reveals anti-correlated networks. Brain Connect. 1, 496–510.

Carolyn, M., Mazure, J.S., 2016. Sex differences in Alzheimer's disease and other dementias. Lancet Neurol. 15, 451.

Celone, K.A., Calhoun, V.D., Dickerson, B.C., Atri, A., Chua, E.F., Miller, S.L., DePeau, K., Rentz, D.M., Selkoe, D.J., Blacker, D., Albert, M.S., Sperling, R.A., 2006. Alterations in memory networks in mild cognitive impairment and Alzheimer's disease: an independent component analysis. J. Neurosci. 26, 10222–10231.

Cisler, J.M., Bush, K., Steele, J.S., 2014. A comparison of statistical methods for detecting context-modulated functional connectivity in fMRI. NeuroImage 84, 1042–1052.

Cohen, A.D., Price, J.C., Weissfeld, L.A., James, J., Rosario, B.L., Bi, W., Nebes, R.D., Saxton, J.A., Snitz, B.E., Aizenstein, H.A., Wolk, D.A., DeKosky, S.T., Mathis, C.A., Klunk, W.E., 2009. Basal cerebral metabolism may modulate the cognitive effects of a beta in mild cognitive impairment: an example of brain reserve. J. Neurosci. 29, 14770–14778.

Cohen, A.D., Mowrey, W., Weissfeld, L.A., Aizenstein, H.J., McDade, E., Mountz, J.M., Nebes, R.D., Saxton, J.A., Snitz, B., Dekosky, S., Williamson, J., Lopez, O.L., Price, J.C., Mathis, C.A., Klunk, W.E., 2013. Classification of amyloid-positivity in controls: comparison of visual read and quantitative approaches. NeuroImage 71, 207–215.

Cook, R.D., 1977. Detection of influential observation in linear regression. Technometrics 19, 15–18.

Dickerson, B.C., Salat, D.H., Bates, J.F., Atiya, M., Killiany, R.J., Greve, D.N., Dale, A.M., Stern, C.E., Blacker, D., Albert, M.S., Sperling, R.A., 2004. Medial temporal lobe function and structure in mild cognitive impairment. Ann. Neurol. 56, 27–35.

Dickerson, B.C., Salat, D.H., Greve, D.N., Chua, E.F., Rand-Giovannetti, E., Rentz, D.M., Bertram, L., Mullin, K., Tanzi, R.E., Blacker, D., Albert, M.S., Sperling, R.A., 2005. Increased hippocampal activation in mild cognitive impairment compared to normal aging and AD. Neurology 65, 404–411.

Duff, S.J., Hampson, E., 2000. A beneficial effect of estrogen on working memory in postmenopausal women taking hormone replacement therapy. Horm. Behav. 38, 262–276.

Dumas, J.A., Kutz, A.M., Naylor, M.R., Johnson, J.V., Newhouse, P.A., 2010. Increased memory load-related frontal activation after estradiol treatment in postmenopausal women. Horm. Behav. 58, 929–935.

Dumitriu, D., Hao, J., Hara, Y., Kaufmann, J., Janssen, W.G.M., Lou, W., Rapp, P.R., Morrison, J.H., 2010. Selective changes in thin spine density and morphology in monkey prefrontal cortex correlate with aging-related cognitive impairment. J. Neurosci. 30, 7507–7515.

Edelman, K., Tudorascu, D., Agudelo, C., Snitz, B., Karim, H., Cohen, A., Mathis, C., Price, J., Weissfeld, L., Klunk, W., Aizenstein, H., 2017. Amyloid-beta deposition is associated with increased medial temporal lobe activation during memory encoding in the cognitively normal elderly. Am. J. Geriatr. Psychiatry 25, 551–560.

Elman, J.A., Oh, H., Madison, C.M., Baker, S.L., Vogel, J.W., Marks, S.M., Crowley, S., O'Neil, J.P., Jagust, W.J., 2014. Neural compensation in older people with brain amyloid-β deposition. Nat. Neurosci. 17, 1316–1318.

Farage, M., Miller, K.W., Zouboulis, C.C., Pierard, G., Maibach, H., 2012. Gender differences in skin aging and the changing profile of the sex hormones with age. J. Steroids Horm 1000109.

Farrer, L.A., Cupples, L.A., Haines, J.L., Hyman, B., Kukull, W.A., Mayeux, R., Myers, R.H., Pericak-Vance, M.A., Risch, N., van Duijn, C.M., 1997. Effects of age, sex, and ethnicity on the association between apolipoprotein E genotype and Alzheimer disease: a meta-analysis. JAMA 278, 1349–1356.

Foster, C.M., Kennedy, K.M., Horn, M.M., Hoagey, D.A., Rodrigue, K.M., 2018. Both hyper- and hypo-activation to cognitive challenge are associated with increased beta-amyloid deposition in healthy aging: a nonlinear effect. NeuroImage 166, 285–292.

Foy, M.R., Baudry, M., Diaz Brinton, R., Thompson, R.F., 2008. Estrogen and hippocampal plasticity in Rodent models. J. Alzheimer's Dis. 15, 589–603.

Friston, K.J., Buechel, C., Fink, G.R., Morris, J., Rolls, E., Dolan, R.J., 1997. Psychophysiological and modulatory interactions in neuroimaging. NeuroImage 6, 218–229.

Grigorova, M., SHERWIN, B., Tulandi, T., 2006. Effects of treatment with leuprolide acetate depot on working memory and executive functions in young premenopausal women. Psychoneuroendocrinology 31, 935–947.

Hämäläinen, A., Pihlajamaki, M., Tanila, H., Hänninen, T., Niskanen, E., Tervo, S., Karjalainen, P.A., Vanninen, R.L., Soininen, H., 2007. Increased fMRI responses during encoding in mild cognitive impairment. Neurobiol. Aging 28, 1889–1903.

Hao, J., Rapp, P.R., Leffler, A.E., Leffler, S.R., Janssen, W.G.M., Lou, W., McKay, H., Roberts, J.A., Wearne, S.L., Hof, P.R., Morrison, J.H., 2006. Estrogen alters spine number and morphology in prefrontal cortex of aged female rhesus monkeys. J. Neurosci. 26, 2571–2578.

Hara, Y., Park, C.S., Janssen, W.G.M., Roberts, M.T., Morrison, J.H., Rapp, P.R., 2012. Synaptic correlates of memory and menopause in the hippocampal dentate gyrus in rhesus monkeys. Neurobiol. Aging 33, 421.e17–421.e28.

Hebert, L.E., Weuve, J., Scherr, P.A., Evans, D.A., 2013. Alzheimer disease in the United States (2010–2050) estimated using the 2010 census. Neurology 80, 1778–1783.

Hedden, T., van Dijk, K.R.A., Becker, J.A., Mehta, A., Sperling, R.A., Johnson, K.A., Buckner, R.L., 2009. Disruption of functional connectivity in clinically normal older adults harboring amyloid burden. J. Neurosci. 29, 12686–12694.

Hoaglin, D.C., Iglewicz, B., Tukey, J.W., 2012. Performance of some resistant rules for outlier labeling. J. Am. Stat. Assoc. 81, 991–999.

Holland, D., Desikan, R.S., Dale, A.M., McEvoy, L.K., 2013. Higher rates of decline for women and apolipoprotein E ε4 carriers. Am. J. Neuroradiology 34, 2287–2293.

Huettel, S.A., Singerman, J.D., Neuroimage, G.M., 2001. The effects of aging upon the hemodynamic response measured by functional MRI. Neuroimage 13, 161–175.

Huijbers, W., Mormino, E.C., Wigman, S.E., Ward, A.M., Vannini, P., McLaren, D.G., Becker, J.A., Schultz, A.P., Hedden, T., Johnson, K.A., Sperling, R.A., 2014. Amyloid deposition is linked to aberrant entorhinal activity among cognitively normal older adults. J. Neurosci. 34, 5200–5210.

Jack Jr., C.R., Knopman, D.S., Jagust, W.J., Shaw, L.M., Aisen, P.S., Weiner, M.W., Petersen, R.C., Trojanowski, J.Q., 2010. Hypothetical model of dynamic biomarkers of the Alzheimer's pathological cascade. Lancet Neurol. 9, 119–128.

Jahani, S., Fantana, A.L., Harper, D., Ellison, J.M., Boas, D.A., Forester, B.P., Yücel, M.A., 2017. fNIRS can robustly measure brain activity during memory encoding and retrieval in healthy subjects. Scientific Rep. 7, 9533.

Kim, M.T., Soussou, W., Gholmieh, G., Ahuja, A., Tanguay, A., Berger, T.W., Brinton, R.D., 2006. 17β-Estradiol potentiates field excitatory postsynaptic potentials within each subfield of the hippocampus with greatest potentiation of the associational/commissural afferents of CA3. Neuroscience 141, 391–406.

Lim, H.K., Nebes, R., Snitz, B., Cohen, A., Mathis, C., Price, J., Weissfeld, L., Klunk, W., Aizenstein, H.J., 2014. Regional amyloid burden and intrinsic connectivity networks in cognitively normal elderly subjects. Brain 137, 3327–3338.

Lin, K.A., Choudhury, K.R., Rathakrishnan, B.G., Marks, D.M., Petrella, J.R., Doraiswamy, P.M., 2015. Marked gender differences in progression of mild cognitive impairment over 8 years. Alzheimer's Dement. Transl. Res. Clin. Interventions 1, 103–110.

Liu, F., Day, M., Muñiz, L.C., Bitran, D., Arias, R., Revilla-Sanchez, R., Grauer, S., Zhang, G., Kelley, C., Pulito, V., Sung, A., Mervis, R.F., Navarra, R., Hirst, W.D., Reinhart, P.H., Marquis, K.L., Moss, S.J., Pangalos, M.N., Brandon, N.J., 2008. Activation of estrogen receptor-|[beta]| regulates hippocampal synaptic plasticity and improves memory. Nat. Neurosci. 11, 334–343.

Lopresti, B.J., Klunk, W.E., Mathis, C.A., Hoge, J.A., Ziolko, S.K., Lu, X.L., Meltzer, C.C., Schimmel, K., Tsopelas, N.D., DeKosky, S.T., Price, J.C., 2005. Simplified quantification of Pittsburgh compound B amyloid imaging PET studies: a comparative analysis. J. Nucl. Med. 46, 1959–1972.

MATLAB, 2015. The MathWorks, Inc., Natick, MA.

Matsumoto, A.M., 2002. Andropause: clinical implications of the decline in serum testosterone levels with aging in men. J. Gerontol. A. Biol. Sci. Med. Sci. 57, M76–M99.

McEwen, B., 2002. Sex, stress and the hippocampus: allostasis, allostatic load and the aging process. Neurobiol. Aging 23, 921–939.

McLaren, D.G., Ries, M.L., Xu, G., Johnson, S.C., 2012. A generalized form of context-dependent psychophysiological interactions (gPPI): a comparison to standard approaches. NeuroImage 61, 1277–1286.

Meltzer, C.C., Zubieta, J.K., Links, J.M., Brakeman, P., Stumpf, M.J., Frost, J.J., 1996. MR-based correction of brain PET measurements for heterogeneous gray matter radioactivity distribution. J. Cereb. Blood Flow Metab. 16, 650–658.

Meltzer, C.C., Smith, G., Price, J.C., Reynolds, C.F., Mathis, C.A., Greer, P., Lopresti, B., Mintun, M.A., Pollock, B.G., Ben-Eliezer, D., Cantwell, M.N., Kaye, W., DeKosky, S.T., 1998. Reduced binding of [18F]altanserin to serotonin type 2A receptors in aging: persistence of effect after partial volume correction. Brain Res. 813, 167–171.

Meltzer, C.C., Cantwell, M.N., Greer, P.J., Ben-Eliezer, D., Smith, G., Frank, G., Kaye, W.H., Houck, P.R., Price, J.C., 2000. Does cerebral blood flow decline in healthy aging? A PET study with partial-volume correction. J. Nucl. Med. 41, 1842–1848.

Mielke, M., Vemuri, P., Rocca, W., 2014. Clinical epidemiology of Alzheimer's disease: assessing sex and gender differences. Clin. Epidemiol. 37.

Miller, S.L., Celone, K., DePeau, K., Diamond, E., Dickerson, B.C., Rentz, D., Pihlajamaki, M., Sperling, R.A., 2008. Age-related memory impairment associated with loss of parietal deactivation but preserved hippocampal activation. PNAS 105, 2181–2186.

Mintun, M.A., LaRossa, G.N., Sheline, Y.I., Dence, C.S., Lee, S.Y., Mach, R.H., Klunk, W.E., Mathis, C.A., DeKosky, S.T., Morris, J.C., 2006. [11C]PIB in a nondemented population Potential antecedent marker of Alzheimer disease. Neurology 67, 446–452.

Mormino, E.C., Smiljic, A., Hayenga, A.O., H Onami, S., Greicius, M.D., Rabinovici, G.D., Janabi, M., Baker, S.L., V Yen, I., Madison, C.M., Miller, B.L., Jagust, W.J., 2011. Relationships between beta-amyloid and functional connectivity in different components of the default mode network in aging. Cereb. Cortex 21, 2399–2407.

Mormino, E.C., Brandel, M.G., Madison, C.M., Marks, S., Baker, S.L., Jagust, W.J., 2012. Aβ deposition in aging is associated with increases in brain activation during successful memory encoding. Cereb. Cortex 22, 1813–1823.

Morrison, J.H., Brinton, R.D., Schmidt, P.J., Gore, A.C., 2006. Estrogen, menopause, and the aging brain: how basic neuroscience can inform hormone therapy in women. J. Neurosci. 26, 10332–10348.

Nebes, R.D., Snitz, B.E., Cohen, A.D., Aizenstein, H.J., Saxton, J.A., Halligan, E.M., Mathis, C.A., Price, J.C., Kamboh, M.I., Weissfeld, L.A., Klunk, W.E., 2013. Cognitive aging in persons with minimal amyloid-β and white matter hyperintensities. Neuropsychologia 51, 2202–2209.

Nichols, T.E., Holmes, A.P., 2002. Nonparametric permutation tests for functional neuroimaging: a primer with examples. Hum. Brain Mapp. 15, 1–25.

Nichols, T.E., Holmes, A.P., 2004. Nonparametric permutation tests for functional neuroimaging. Hum. Brain Funct. 46, 887–910.

Nyberg, L., 2016. Functional brain imaging of episodic memory decline in ageing. J. Intern. Med. 281, 65–74.

O'brien, J.L., O'keefe, K.M., LaViolette, P.S., DeLuca, A.N., Blacker, D., Dickerson, B.C., Sperling, R.A., 2010. Longitudinal fMRI in elderly reveals loss of hippocampal activation with clinical decline. Neurology 74, 1969–1976.

Oh, H., Jagust, W.J., 2013. Frontotemporal network connectivity during memory encoding is increased with aging and disrupted by beta-amyloid. J. Neurosci. 33, 18425–18437.

Patel, A.X., Kundu, P., Rubinov, M., Jones, P.S., V rtes, P.E., Ersche, K.D., Suckling, J., Bullmore, E.T., 2014. A wavelet method for modeling and despiking motion artifacts from resting-state fMRI time series. NeuroImage 95, 287–304.

Payami, H., Montee, K.R., Kaye, J.A., Bird, T.D., Yu, C.-E., Wijsman, E.M., Schellenberg, G.D., 1994. Alzheimer's disease, apolipoprotein E4, and gender. JAMA 271, 1316–1317.

Perrin, R.J., Fagan, A.M., Holtzman, D.M., 2009. Multimodal techniques for diagnosis and prognosis of Alzheimer's disease. Nature 461, 916–922.

Petersen, R.C., Roberts, R.O., Knopman, D.S., Geda, Y.E., Cha, R.H., Pankratz, V.S., Boeve, B.F., Tangalos, E.G., Ivnik, R.J., Rocca, W.A., 2010. Prevalence of mild cognitive impairment is higher in men the Mayo Clinic Study of Aging. Neurology 75, 889–897.

Pizzi, S.D., Punzi, M., Sensi, S.L., 2018. Functional signature of conversion in mild cognitive impairment patients. bioRxiv 290783.

Poirier, J., Bertrand, P., Kogan, S., Gauthier, S., Davignon, J., Bouthillier, D., 1993. Apolipoprotein E polymorphism and Alzheimer's disease. Lancet 342, 697–699.

Price, J.C., Klunk, W.E., Lopresti, B.J., Lu, X., Hoge, J.A., Ziolko, S.K., Holt, D.P., Meltzer, C.C., DeKosky, S.T., Mathis, C.A., 2005. Kinetic modeling of amyloid binding in humans using PET imaging and Pittsburgh compound-B. J. Cereb. Blood Flow Metab. 25, 1528–1547.

Rapp, P.R., Morrison, J.H., Roberts, J.A., 2003. Cyclic estrogen replacement improves cognitive function in aged ovariectomized rhesus monkeys. J. Neurosci. 23, 5708–5714.

Roberts, R.O., Geda, Y.E., Knopman, D.S., Cha, R.H., Pankratz, V.S., Boeve, B.F., Tangalos, E.G., Ivnik, R.J., Rocca, W.A., Petersen, R.C., 2012. The incidence of MCI differs by subtype and is higher in men the Mayo Clinic Study of Aging. Neurology 78, 342–351.

Salami, A., Pudas, S., Nyberg, L., 2014. Elevated hippocampal resting-state connectivity underlies deficient neurocognitive function in aging. PNAS 111, 17654–17659.

Schultz, A.P., Chhatwal, J.P., Hedden, T., Mormino, E.C., Hanseeuw, B.J., Sepulcre, J., Huijbers, W., LaPoint, M., Buckley, R.F., Johnson, K.A., Sperling, R.A., 2017. Phases of hyperconnectivity and hypoconnectivity in the default mode and salience networks track with amyloid and Tau in clinically normal individuals. J. Neurosci. 37, 4323–4331.

Schulz, K., Korz, V., 2010. Hippocampal testosterone relates to reference memory performance and synaptic plasticity in male rats. Front. Behav. Neurosci. 4.

Shaywitz, S.E., Shaywitz, B.A., Pugh, K.R., Fulbright, R.K., Skudlarski, P., Mencl, W.E., Constable, R.T., Naftolin, F., Palter, S.F., Marchione, K.E., Katz, L., Shankweiler, D.P., Fletcher, J.M., Lacadie, C., Keltz, M., Gore, J.C., 1999. Effect of estrogen on brain activation patterns in postmenopausal women during working memory tasks. JAMA 281, 1197–1202.

Sheline, Y.I., Raichle, M.E., Snyder, A.Z., Morris, J.C., Head, D., Wang, S., Mintun, M.A., 2010. Amyloid plaques disrupt resting state default mode network connectivity in cognitively normal elderly. Biol. Psychiatry 67, 584–587.

Snyder, P.J., 2017. Overview of Testosterone Deficiency in Older Men. https://www.uptodate.com/contents/overview-of-testosterone-deficiency-in-older-men#H28. (Accessed 9 October 2017).

Sperling, R., 2011. The potential of functional MRI as a biomarker in early Alzheimer's disease. Neurobiol. Aging 32, S37–S43.

Sperling, R., Chua, E., Cocchiarella, A., Rand-Giovannetti, E., Poldrack, R., Schacter, D.L., Albert, M., 2003. Putting names to faces: NeuroImage 20, 1400–1410.

Sperling, R.A., Bates, J.F., Chua, E.F., Cocchiarella, A.J., Rentz, D.M., Rosen, B.R., Schacter, D.L., Albert, M.S., 2003a. fMRI studies of associative encoding in young and elderly controls and mild Alzheimer's disease. J. Neurol. Neurosurg. Psychiatry 74, 44–50.

Sperling, R.A., LaViolette, P.S., O'Keefe, K., O'Brien, J., Rentz, D.M., Pihlajamaki, M., Marshall, G., Hyman, B.T., Selkoe, D.J., Hedden, T., Buckner, R.L., Becker, J.A., Johnson, K.A., 2009. Amyloid deposition is associated with impaired default network function in older persons without dementia. Neuron 63, 178–188.

Sperling, R.A., Aisen, P.S., Beckett, L.A., Bennett, D.A., Craft, S., Fagan, A.M., Iwatsubo, T., Jack Jr, C.R., Kaye, J., Montine, T.J., Park, D.C., Reiman, E.M., Rowe, C.C., Siemers, E., Stern, Y., Yaffe, K., Carrillo, M.C., Thies, B., Morrison-Bogorad, M., Wagster, M.V., Phelps, C.H., Iwatsubo, T., Jack Jr, C.R., Kaye, J., Montine, T.J., Park, D.C., Reiman, E.M., Rowe, C.C., Siemers, E., Stern, Y., Yaffe, K., Carrillo, M.C., Thies, B., Morrison-Bogorad, M., Wagster, M.V., Phelps, C.H., 2011. Toward defining the preclinical stages of Alzheimer's disease: recommendations from the National Institute on Aging-Alzheimer's Association workgroups on diagnostic guidelines for Alzheimer's disease. Alzheimer's Dement. 7, 280–292.

Tzourio-Mazoyer, N., Landeau, B., Papathanassiou, D., Crivello, F., Etard, O., Delcroix, N., Mazoyer, B., Joliot, M., 2002. Automated anatomical labeling of activations in SPM using a macroscopic anatomical parcellation of the MNI MRI single-subject brain. NeuroImage 15, 273–289.

Vannini, P., Hedden, T., Becker, J.A., Sullivan, C., Putcha, D., Rentz, D., Johnson, K.A., Sperling, R.A., 2012. Age and amyloid-related alterations in default network habituation to stimulus repetition. Neurobiol. Aging 33, 1237–1252.

Wang, A.C.J., Hara, Y., Janssen, W.G.M., Rapp, P.R., Morrison, J.H., 2010. Synaptic estrogen receptor-α levels in prefrontal cortex in female rhesus monkeys and their correlation with cognitive performance. J. Neurosci. 30, 12770–12776.

Wilson, A.A., Garcia, A., Jin, L., Houle, S., 2000. Radiotracer synthesis from [^{11}C]-iodomethane: a remarkably simple captive solvent method. Nucl. Med. Biol. 27, 529–532.

Woods, R.P., Mazziotta, J.C., Cherry, S.R., 1993. MRI-PET registration with automated algorithm. J. Comput. Assist. Tomogr. 17, 536–546.

Woolley, C.S., McEwen, B.S., 1993. Roles of estradiol and progesterone in regulation of hippocampal dendritic spine density during the estrous cycle in the rat. J. Comp. Neurol. 336, 293–306.

Woolley, C.S., Gould, E., Frankfurt, M., McEwen, B.S., 1990. Naturally occurring fluctuation in dendritic spine density on adult hippocampal pyramidal neurons. J. Neurosci. 10, 4035–4039.

Zeineh, M.M., Engel, S.A., Thompson, P.M., Bookheimer, S.Y., 2003. Dynamics of the Hippocampus during encoding and retrieval of face-name pairs. Science 299, 577–580.

Zhang, Q.-G., Wang, R.-M., Scott, E., Han, D., Dong, Y., Tu, J.-Y., Yang, F., Reddy Sareddy, G., Vadlamudi, R.K., Brann, D.W., 2013. Hypersensitivity of the hippocampal CA3 region to stress-induced neurodegeneration and amyloidogenesis in a rat model of surgical menopause. Brain 136, 1432–1445.

Zhou, Z., Ding, M., Chen, Y., Wright, P., Lu, Z., Liu, Y., 2009. Detecting directional influence in fMRI connectivity analysis using PCA based Granger causality. Brain Res. 1289, 22–29.